J Arid Land (2024) 16(10): 1344–1364
doi: 10.1007/s40333-024-0108-x; CSTR: 32276.14.JAL.0240108x

Science Press Springer-Verlag

Spatial distribution of soil salinization under the influence of human activities in arid areas, China

LIU Yufang[1], YANG Qingwen[1,2*], PEI Xiangjun[1,2], LI Jingji[1,2], WANG Shuangcheng[3], HUANG Zhenfu[3], HAN Wei[3], ZHENG Tianliang[1,2]

[1] College of Ecology and Environment, Chengdu University of Technology, Chengdu 610059, China;
[2] Tianfu Yongxing Laboratory, Chengdu 610213, China;
[3] Hydrogeological and Engineering Geological Team of Xinjiang Bureau of Geo-Exploration & Mineral Development, Changji 831100, China

Abstract: The Hotan Prefecture of Xinjiang Uygur Autonomous Region, China belongs to arid desert climate, with significant soil salinization issues. The study selected six rivers in Hotan Prefecture (Pishan, Qaraqash, Yurungqash, Celle, Kriya, and Niya rivers) to explore the spatial distribution of soil salinization in this area and its underlying mechanisms. Sampling was conducted along each river's watershed, from the Gobi in the upper reaches, through the anthropogenic impact area in the middle reaches, to the desert area in the lower reaches. Soil physical-chemical indicators, including total soluble salts, pH, K^+, Na^+, Ca^{2+}, Mg^{2+}, SO_4^{2-}, Cl^-, CO_3^{2-}, HCO_3^-, organic matter, available nitrogen, available phosphorus, and available potassium, were tested, along with the total dissolved solids of surface water and groundwater. The results revealed that the soil water and nutrient contents in anthropogenic impact area were higher than those in Gobi and desert areas, while the pH and total soluble salts were lower than those in Gobi and desert areas. The ions in the soil of the study area were primarily Cl^-, SO_4^{2-}, K^+, and Na^+, and the ion concentration of soil salt were positively correlated with surface water and groundwater. Overall, the study area exhibited low soil water content, low clay content, infertile soil, and high soil salinization, dominated by weak to moderate chloride-sulfate types. Compared with Gobi and desert areas, the soil in anthropogenic impact area had higher soil water content, lower pH, lower soluble salts, and higher nutrients, indicating that human farming activities help mitigate salinization. These findings have practical implications for guiding the scientific prevention and control of soil salinization in the arid areas and for promoting sustainable agricultural development.

Keywords: soil salinization; human activities; spatial distribution; Hotan Prefecture; soil soluble salt; soil nutrient

Citation: LIU Yufang, YANG Qingwen, PEI Xiangjun, LI Jingji, WANG Shuangcheng, HUANG Zhenfu, HAN Wei, ZHENG Tianliang. 2024. Spatial distribution of soil salinization under the influence of human activities in arid areas, China. Journal of Arid Land, 16(10): 1344–1364. https://doi.org/10.1007/s40333-024-0108-x; http://cstr.cn/32276.14.JAL.0240108x

1 Introduction

Soil salinization is a global environmental issue, primarily affecting the natural arid and semi-arid areas of Africa, Asia, and Latin America. In China, it mainly occurs in the coastal area, the Northeast China, and the inland arid area of Northwest China. Soil salinization can cause soil crusting and reduce crop yield and quality (Daliakopoulos et al., 2016; Scanlon et al., 2010a, b). Land salinization in arid areas is particularly challenging to combat. This is mainly due to the high

*Corresponding author: YANG Qingwen (yangqingwen20@cdut.edu.cn)
Received 2024-06-02; revised 2024-09-25; accepted 2024-09-30

variety and content of soluble salts in the soil-forming parent rock, coupled with the combined effects of high groundwater mineralization, an arid climate with little precipitation, underdeveloped crop planting systems, and irrational human activities, accelerating soil salinization (Jiang et al., 2019; Perri et al., 2020; Shokri-Kuehni et al., 2020; Yin et al., 2022; Yu et al., 2022).

Xinjiang Uygur Autonomous Region (hereinafter referred to as Xinjiang) is one of the regions most affected by soil salinization in both China and globally, due to its location in the heart of the Eurasian continent (Bai et al., 2023), inland arid climate, and limited water resources. The region has distinct geographical features, with a landscape covering a complex mix of mountains, Gobi, deserts, and oases. Most areas have sparse vegetation due to harsh natural conditions, alongside strong evaporation and high levels of land salinization. The southern part of Xinjiang (hereinafter referred to as southern Xinjiang) experiences more severe soil salinization than the northern part. Water scarcity and soil salinization are two major constraints to sustainable agricultural development in the oasis zones and to maintaining vegetation stability in the desert-intertwined zones of Xinjiang (Li et al., 2016a). Soil salinization in Xinjiang can be attributed to both natural factors and human activities. Among the natural factors, climatic drivers are the key energy sources influencing soil salinization in this region (Zhuang et al., 2021a; Li et al., 2022; Yin et al., 2022). The rock and soil matrices in Xinjiang's mountainous areas are typically rich in salts, including insoluble carbonates and gypsum, as well as soluble chloride-sulfate components. In particular, in the mountainous foreland of Hotan Prefecture, soil salinity can reach 50–900 g/kg (Tian et al., 2000; Yin et al., 2022). Additionally, the combination of highly mineralized groundwater and the extremely arid desert climate has exacerbated the salinization problem (Yin et al., 2022). On the other hand, human activities, especially irrational agricultural practices such as excessive groundwater extraction for irrigation, have significantly worsened soil salinization. While excessive groundwater extraction initially washes away salts from the soil's surface, subsequent evaporation causes these salts to gradually accumulate and migrate back to the surface, worsening salinization conditions (Liu et al., 2018; Perri et al., 2018; Fan et al., 2020). Among all contributing factors, human activities hold the greatest potential for regulation, making them crucial in the control of salinization.

Currently, the existing salinization prevention and control technologies are primarily focused on identifying the type and degree of soil salinization to implement strategies such as engineering salt leaching, the application of organic matter (OM) and chemical substances, and the planting of salt-tolerant or salt-absorbing plants to regulate the water-salt balance in the soil (Zeng et al., 2014; Wang et al., 2017; Liu et al., 2018; Zheng et al., 2018; He et al., 2020; Wang et al., 2021c; Du et al., 2023). Understanding the spatial distribution pattern and formation mechanisms of salinity is crucial for evaluating the effectiveness of salinity prevention and control measures. An in-depth investigation into the intrinsic laws governing the spatial distribution of salinity and its generation mechanisms is critical for guiding targeted salinity prevention and control practices. However, systematic research on the spatial distribution of soil salinization, especially under the comprehensive influence and spatial response to various human activities in southern Xinjiang, remains insufficient.

In this study, the Hotan Prefecture of southern Xinjiang, where soil salinization is highly prominent, was taken as a case study. We analyzed the spatial distribution pattern of saline soils through *in situ* investigation, sampling, indoor testing, and the analysis of physical indices such as soil water content, electrical conductivity (EC), permeability coefficient, particle size gradation, and chemical indices such as soluble salt anions and cations, organic matter (OM), available nitrogen (AN), available phosphorus (AP), and available potassium (AK). We also explored the mechanisms behind the formation of saline soils and their distribution response to the impacts of human activities. The findings of this study might provide theoretical guidance for the zoning and grading management of salinized land in Hotan Prefecture.

2 Study area

The study area is located in the Hotan Prefecture of Xinjiang (36°16′07″–38°37′04″N, 77°39′51″–84°54′58″E), bordered by the Tarim Basin to the north and the Kunlun Mountains to the south, with the topography sloping from high in the southwest to low in the northeast. The main landform types, moving from west to east, include mountains, woodlands, Gobi, oases, and deserts. Six rivers, namely the Pishan, Qaraqash, Yurungqash, Celle, Kriya, and Niya rivers, flow from south to north. The average annual temperature in Hotan Prefecture is 12.5°C, the average annual precipitation is less than 50 mm, and the annual evaporation exceeds 2600 mm (Zhang, 2023). Water resources are unevenly distributed in terms of time, space, and geography, leading to serious constraints on agricultural development.

3 Survey and test methods

3.1 Sample collection

The primary investigation area was the oasis zone with human habitation, and line sampling was conducted along the rivers in Hotan Prefecture. Sampling sites were located in the upper reaches and lower reaches of the six rivers (Pishan, Qaraqash, Yurungqash, Celle, Kriya, and Niya rivers), spanning Gobi, desert, artificial oases, and desert landscapes. Due to the presence of alpine meadows in the upper reaches of the study area, we conducted a field survey across all geomorphological types throughout the watershed.

We conducted sampling in May–July 2023. In selecting sampling sites, factors such as the uniformity of spatial distribution, transportation accessibility, and others were considered. This study set 159 soil sample collection sites (Fig. 1). These sites included 19 sites along the Pishan River, 55 along the Qaraqash River, 34 along the Yurungqash River, 15 along the Celle River, 24 along the Kriya River, and 12 along the Niya River Basin.

At each site, five subsample points were identified for collection using a double diagonal pattern centered on a 10 m×10 m plot. Soil samples were taken in layers at depths of 0–50 cm, with intervals of 10 cm between sampling depths. Soil samples from the same depth at different subsample points within the plot were mixed to form a composite sample representing soil conditions at each site. A portion of these soil samples was placed in aluminum boxes and returned to the laboratory for moisture content testing using the drying method. The remaining soil samples were collected in sampling bags and transported to the laboratory for testing of other physical and chemical soil properties.

Additionally, the ecological and geological sensitivity of various sections and the degree of desertification of the surrounding land were considered. We selected 37 surface water sites for sampling: 11 along the Yurungqash River, 7 along the Qaraqash River, 8 along the Kriya River, 5 along the Niya River, 3 along the Pishan River, and 3 along the Celle River. In addition, this study collected 58 sets of shallow groundwater (mainly came from the shallow quaternary pore aquifer system) quality data, which were gathered by the project "1:100,000 Hydrogeological and Environmental Geological Survey of Hotan-Pishan Area, Xinjiang". In total, 159 groups of soil samples and 37 groups of water samples were collected, with the specific distribution shown in Figure 1.

3.2 Sample processing

The technical requirements for surface water sample collection refer to the Technical Specifications Requirements for Monitoring of Surface Water and Waste Water (Ministry of Ecology and Environment of the People's Republic of China, 2002). The water was collected using a needle removal syringe and passed through a 0.45-μm filter membrane into a 50-mL polyethylene terephthalate (PET) sampling bottle for anion testing. Another 50 mL of water was collected and acidified with 250 μL of excellent pure nitric acid in a cation sampling bottle. The samples were stored at 4°C and transported back to the laboratory for testing as soon as possible.

Soil samples collected from the field were promptly placed in porcelain trays. Stones, plant residues, and other non-soil components were carefully removed from the fresh soil samples using tweezers. The cleaned samples were then immediately placed in self-sealing bags, sealed for

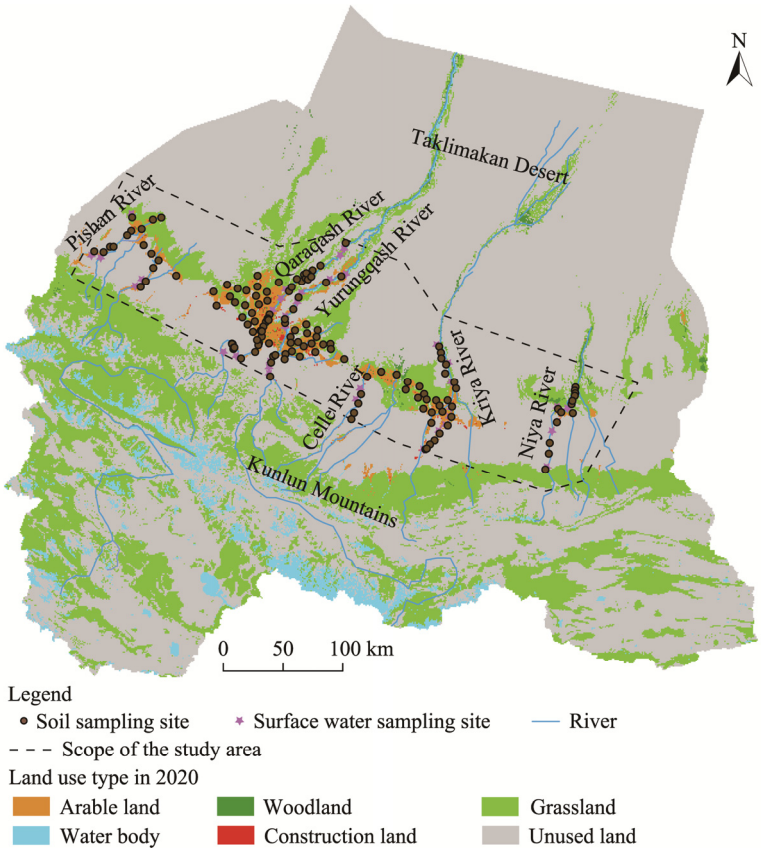

Fig. 1 Spatial distribution of sampling sites in the study area

preservation, and stored until subsequent indicator tests were conducted. The soil samples after removing impurities and drying were used to measure SWC, while the soil samples after air-drying, grinding, and sieving through 2-mm mesh were used for testing gradation. A laser particle size analyzer (MS-S, British Malvern Instrument, Malvern, UK) was then used to measure soil gradation. The remaining soil samples were spread to a thickness of 2–3 cm, left to dry naturally in a well-ventilated space, and frequently turned during the air-drying process to accelerate drying. The air-dried samples were used to measure other indices, including total soluble salts, pH, and the concentrations of K^+, Na^+, Ca^{2+}, Mg^{2+}, SO_4^{2-}, Cl^-, CO_3^{2-}, HCO_3^-, OM, AN, AP, and AK.

3.3 Test methods

The pH, total dissolved solids (TDS), and the concentration of K^+, Na^+, Ca^{2+}, Mg^{2+}, SO_4^{2-}, Cl^-, and HCO_3^- of water samples were tested by the methods of the Standards for Drinking Water Quality (National Health Commission of the People's Republic of China, 2006).

Soil water content and bulk weight were determined using the oven-drying method, where soil samples were dried at 105°C for 48 h until reaching a constant weight. The formulas used for these calculations are presented in Equations 1 and 2 (Zhao, 1981). The pH was measured using a pH meter (Mettler Toledo S40, Mettler Toledo International Ltd., Shanghai, China) with an accuracy of 0.01, and EC was measured using a portable conductivity meter (Leici DDSJ-308F, Mettler Toledo International Ltd., Shanghai, China) (Chen et al., 2017). The soil permeability coefficient was determined using a TST-55 variable-head permeability meter (Nanjing Soil Instrument Factory Ltd.

(NSIF), Nanjing, China). For particle size gradation analysis, soil particles smaller than 2 mm were screened and tested using a laser particle sizer.

The formula for water content calculation is as follows:

$$w = (\frac{m_0}{m_d} - 1) \times 100\%, \tag{1}$$

where w is the water content (%); m_0 is the mass of wet soil (g); and m_d is the mass of dry soil (g).

The formula for bulk density calculation is as follows:

$$\rho = \frac{m - m_1}{v}, \tag{2}$$

where ρ is the bulk density (g/cm^3); m is the sum of the dry weight of the soil and the mass of the ring cutter (g); m_1 is the mass of the ring cutter (g); and v is the volume of the ring cutter (cm^3).

The formula for permeability coefficient calculation is as follows:

$$K_T = 2.3 \frac{aL}{At} \lg \frac{H_{b1}}{H_{b2}}, \tag{3}$$

where K_T is the permeability coefficient (cm/s); a is the area of the cross-sectional zone of the variable-head pipe (cm^2); L is the seepage diameter (cm); A is the surface area of the specimen (cm^2); t is the time duration (s); H_{b1} is the liquid level at the beginning (cm); and H_{b2} is the liquid level at the termination (cm).

We determined the salt ion concentrations based on the soil diluted extract method. Total soluble salts were analyzed by forest soil water-soluble salt analysis. The K^+ and Na^+ concentrations were measured by flame photometry, while the Ca^{2+} and Mg^{2+} concentrations were determined by an ethylene diamine tetraacetic acid (EDTA) complexometric titration, the Cl^- concentration was determined by a silver nitrate titration, the SO_4^{2-} concentration was determined by an EDTA complexometric titration, and the CO_3^{2-} and HCO_3^- concentrations were determined by the acid-alkali neutralization titrimetric method (with a pH of about 4.8) (Yang et al., 2014; Chen et al., 2019).

The soil AN content was determined by the alkaline hydrolysis diffusion method. The AP content of the soil samples was determined by the sodium hydrogen carbonate solution-Mo-Sb anti spectrophotometric method. The soil AK content was determined by the ammonium acetate flame photometer method. And the soil OM was determined by potassium dichromate method (Zhao, 2018).

The specific methods used for each indicator are listed in Table 1. All tests were conducted with three parallel groups for each sample.

3.4 Data processing

Based on land use data from the China Land Cover Dataset (Wuhan University National Land Use Interpretation; http://www.ncdc.ac.cn) (Yang and Huang, 2021), we classified the land use types in Hotan Prefecture into six categories: arable land, woodland, grassland, water body, construction land, and unused land. A spatial distribution database of soil properties for the study area was constructed by combining field-collected soil sample sites with corresponding test results. Following a previous study (Zheng et al., 2024), three indicators were selected for this study: land use type, population density, and nighttime light. These indicators were used to calculate the intensity of human activities in the study area, with a higher score for the human footprint index (HF) indicating a greater impact of human activities.

The HF is calculated using the following formula (Zheng et al., 2024):

$$\mathrm{HF} = I_{\mathrm{LUCC}} + I_{\mathrm{POP}} + I_{\mathrm{NL}}, \tag{4}$$

where HF is the human footprint index within the image range, with value ranging 0–30; I_{LUCC} is the intensity of the impact of land use type within the image range, with value ranging 0–10; I_{POP} is the intensity of the impact of population density within the image range, with value ranging 0–10; and I_{NL} is the intensity of the impact of nighttime light within the image range, with value ranging 0–10. The higher the HF value, the greater the human activity intensity.

Table 1 Assigned value of each indicator in this study

Indicator	Classification	Assigned value
Land use type	Construction land	10
	Arable land	7
	Woodland	5
	Grassland	3
	Water body	2
	Unused land	1
Population density (persons/km^2)	>1200	10
	250–1200	7
	70–250	5
	30–70	2
	0–30	1
Nighttime light (nW/(cm^2·sr))	75.0–160.0	10
	40.0–75.0	7
	24.0–40.0	5
	10.0–24.0	3
	4.6–10.0	2
	0.0–4.6	1

Note: The assigned value to each indicator was referred from Duan and Luo (2021).

The population data for this analysis were sourced from the Resources and Environmental Science Data Center (http://www.resdc.cn/) and the nighttime light data were from National Polar-orbiting Partnership/Visible Infrared Imaging Radiometer Suite (NPP /VIIRS; https://eogdata.mines.edu/products/dmsp/#monthly). Using the geostatistical analysis module within geographic information system (GIS) software, ordinary Kriging was employed to differentiate levels of anthropogenic impact across the study area. We categorized the intensity of anthropogenic activities according to HF values as follows: Gobi and desert areas without anthropogenic activities ($0<HF<2$); mildly impacted by anthropogenic activities ($2\leq HF<9$); and severely impacted by anthropogenic activities ($9\leq HF<30$). The spatial distribution of soil physicochemical properties in Hotan Prefecture was analyzed under the influence of various watershed units and anthropogenic activities.

For the data processing of all soil physical and chemical indicators, Origin 2021 software (OriginLab, Northampton, Masaachusetts, USA) was utilized. The Pearson correlation coefficient was used to reflect correlations between soil nutrients and major salt-based ion indicators.

4 Results

4.1 Changes in surface water-groundwater salinity

The pH of the groundwater system in the study area ranged from 7.05 to 8.86, with a mean value of 8.04, and was generally weakly alkaline (Table 2). The TDS varied from 654.70 to 3338.92 mg/L, with a mean value of 1270.00 mg/L, and most of the water was brackish. The pH value of surface water ranged from 7.63 to 8.80, with a mean value of 8.32, which was weakly alkaline. Na^+ was the dominant cation in river water ions, ranging from 31.70 to 1957.00 mg/L. The TDS distribution of the surface water in the study area exhibited high salinization characteristics (Fig. 2). The value of TDS varied significantly across the entire basin, ranging from 288.00 to 9135.00 mg/L and with an average value of 1325.36 mg/L. This average was much higher than the average levels found in global semi-arid and arid areas, and it was more pronounced in the Yurungqash and Qaraqash river basins.

Table 2 Results of hydro-chemical parameters of surface water and groundwater in the study area

Type	Statistical indicator	pH	Concentration (mg/L)							
			TDS	K^+	Na^+	Ca^{2+}	Mg^{2+}	Cl^-	SO_4^{2-}	HCO_3^-
Groundwater	Min	7.05	654.70	10.65	91.36	11.63	24.09	137.57	13.01	58.67
	Max	8.86	3338.92	59.58	698.38	192.58	275.41	1134.63	1095.96	549.51
	Average	8.04	1270.00	21.70	265.24	78.10	66.59	374.65	310.21	310.94
	SD	0.40	662.08	9.68	159.07	33.59	45.08	257.01	225.94	110.94
Surface water	Min	7.63	288.00	2.18	38.10	31.70	10.50	35.40	75.70	5.72
	Max	8.80	9135.00	138.00	449.00	1957.00	336.00	4297.00	2589.00	3097.00
	Average	8.32	1325.36	15.70	85.50	229.00	49.00	359.00	467.00	494.00
	SD	0.29	1453.74	54.59	68.90	310.42	54.59	663.00	609.78	618.48

Note: TDS, total dissolved solids; Min, minimum value; Max, maximum value; SD, standard deviation.

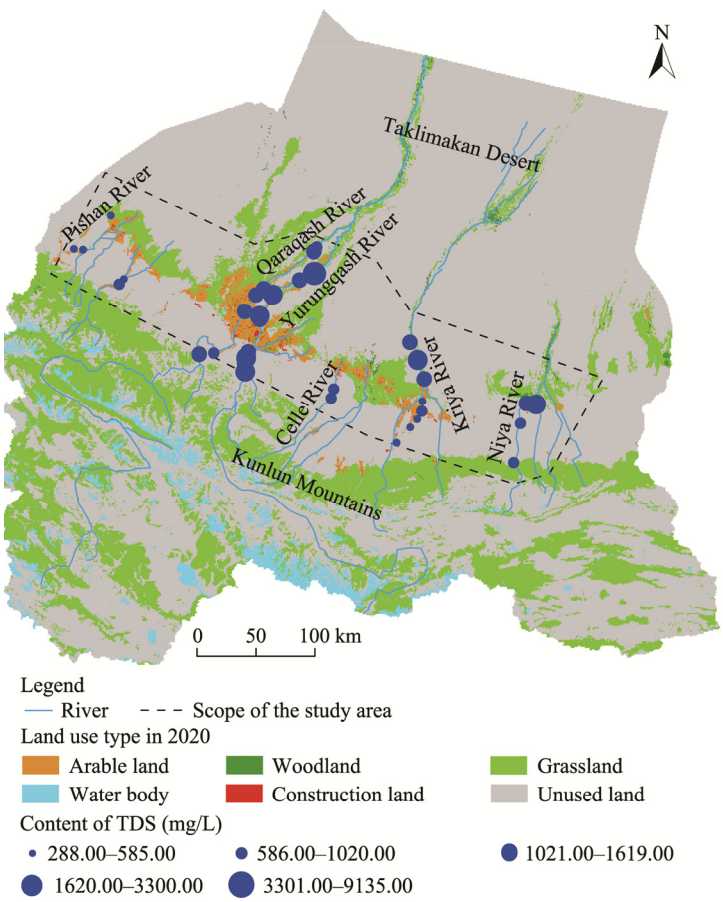

Fig. 2 Spatial distribution of the total dissolved solids (TDS) of surface water in the study area

4.2 Changes in soil physical and chemical properties

Figures 3 and 4 show the spatial distribution of soil physical-chemical parameters (water content, infiltration coefficient, natural bulk density, and dry bulk density) in the study area, along with box plots of the average water content in different basins. From Figures 3a and 4a, it is evident that the soil water content in anthropogenic impact area was significantly higher than those in Gobi and desert areas, as indicated by the following ranking: severely affected area of human

activities>mildly affected area of human activities>Gobi≥desert. Furthermore, a comparison of different watersheds revealed that the sample sites with high soil water content were primarily located in the severely affected area of Yurungqash River Basin and Qaraqash River Basin, which had an average soil water content of about 23.24%. In contrast, the Gobi and desert areas exhibited very low soil water content. The soil water content rose to approximately 15.50% in the Kriya and Niya river basins as they transitioned from Gobi to anthropogenic impact area. The Pishan River and Celle River basins, however, demonstrated an increasing trend of soil water content from south to north. Overall, the soil water content in the study area exhibited a spatial distribution pattern characterized by higher values in the center and lower values in the surrounding areas (Fig. 3a).

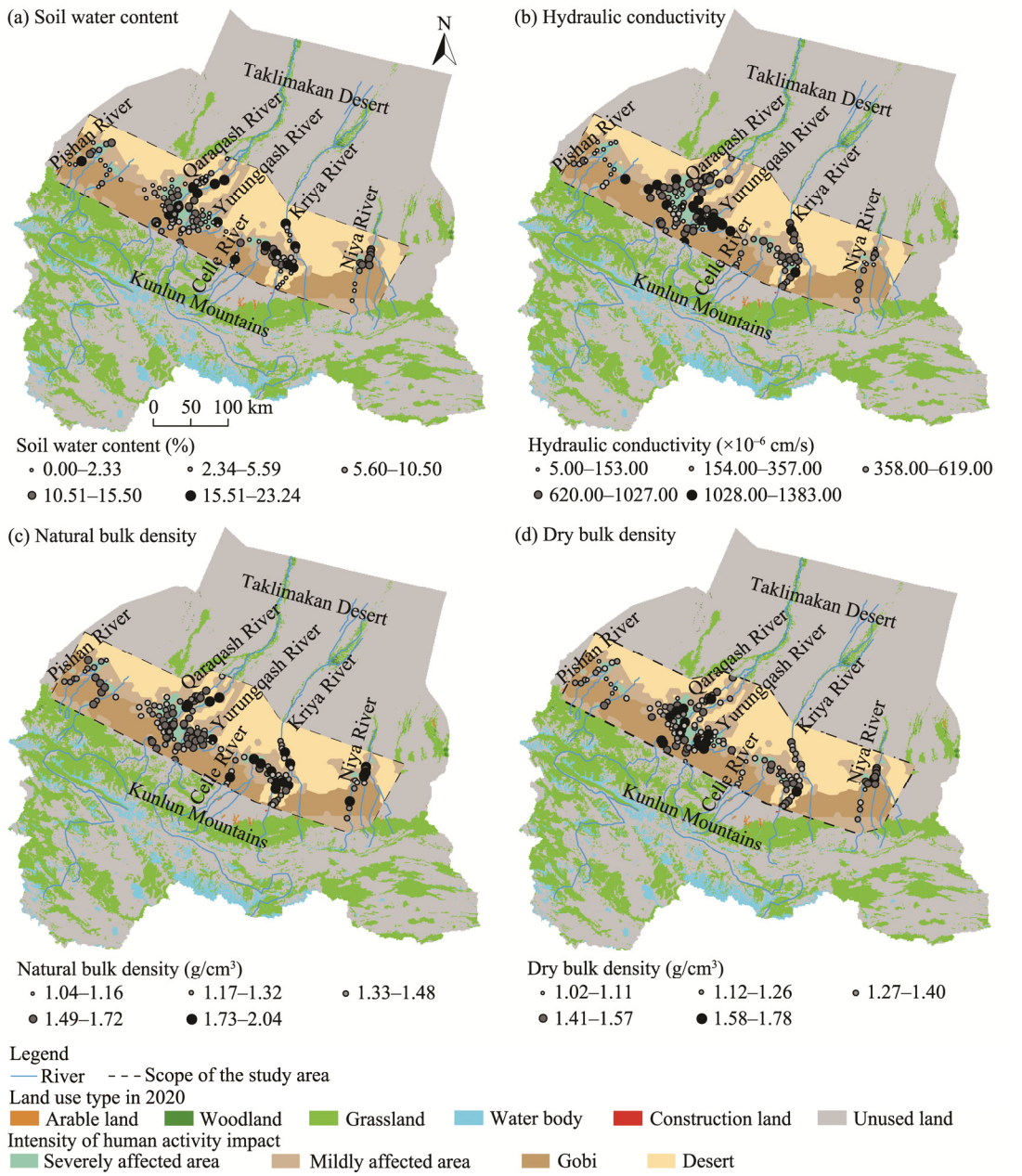

Fig. 3 Spatial distribution of soil physical and chemical property parameters in the study area. (a), soil water content; (b), hydraulic conductivity; (c), natural bulk density; (d), dry bulk density.

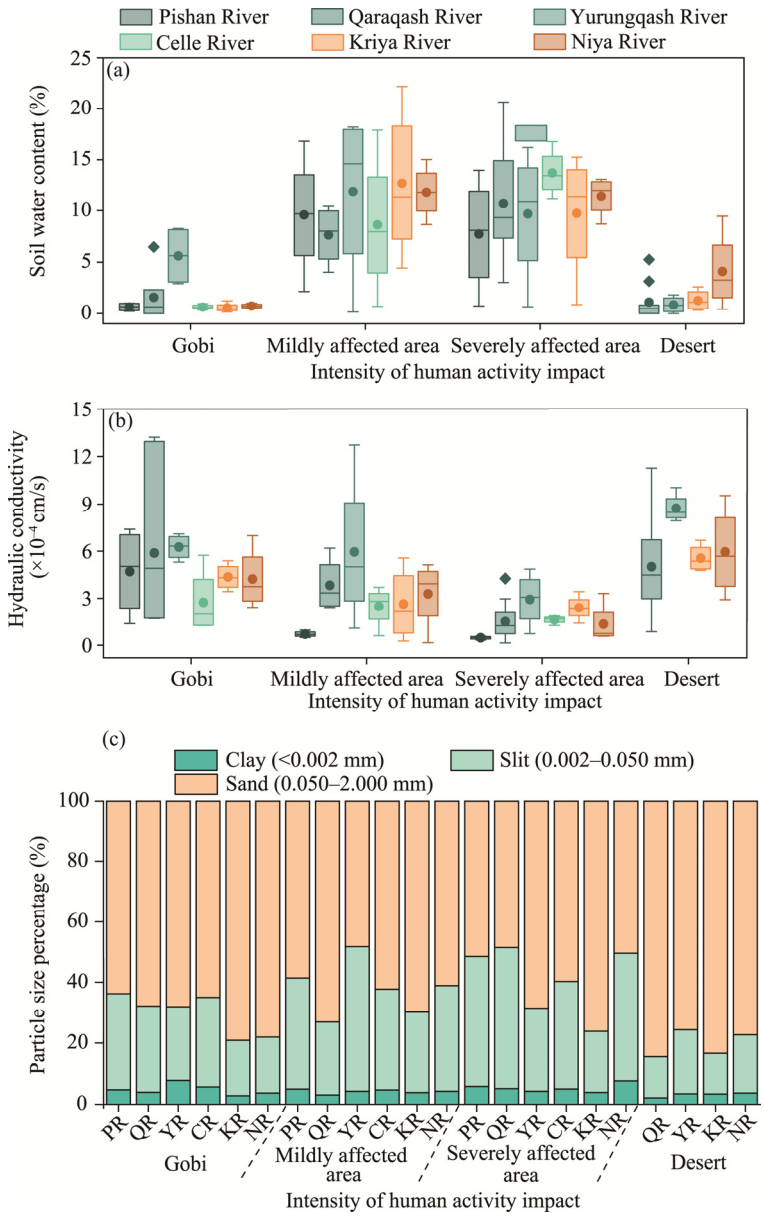

Fig. 4 Change in soil physical and chemical property parameters in typical watersheds of the study area. (a), soil water content; (b), particle size percentage; (c) hydraulic conductivity. The upper and lower limits of the box plots represent the maximum and minimum values, the middle line represents median, the origin represents arithmetic mean, and the diamond-shaped block represents outlier. PR, Pishan River; QR, Qaraqash River; YR, Yurungqash River; CR, Celle River; KR, Kriya River; NR, Niya River.

From Figures 3b and 4c, it can be observed that the hydraulic conductivity was directly influenced by particle size distribution. The mean value of the hydraulic conductivity was larger in Gobi area and desert area; in the severely affected area of Yurungqash and Qaraqash river basins, the hydraulic conductivity ranged from 4.62×10^{-6} to 1.53×10^{-4} cm/s. This lower hydraulic conductivity may be attributed to improved soil structure. Overall, the mean value of hydraulic conductivity was smaller in severely affected area (approximately 1.54×10^{-4}–3.57×10^{-4} cm/s) and larger in Gobi area and desert area, reaching up to 1.38×10^{-3} cm/s.

Figure 3c illustrates that the natural bulk density and water content of soils in the basin scale exhibited similar patterns, with the bulk density in severely affected area being higher than that in

Gobi and desert areas, reaching a maximum value of 2.04 g/cm^3. Conversely, the dry bulk density of soils in areas impacted by human activities (1.02–1.26 g/cm^3) was lower than those in Gobi (1.41–1.78 g/cm^3) and desert (1.27–1.57 g/cm^3) areas (Fig. 3d). Additionally, significant variations in dry bulk density were observed among the basin units; sample sites in the Yurungqash, Qaraqash, and Kriya river basins located away from the severely affected area exhibited high dry bulk density, while the Pishan and Celle river basins displayed a decreasing trend in dry bulk density from south to north.

The soils in the study area, as shown in Figure 4c, were predominantly composed of slit (20.60%) and sand (62.70%), which together accounted for over 80.00% of the total composition, whereas clay content was less than 20.00%. In each watershed unit, the order of clay content was as follows: highest in severely affected area, lowest in desert area, and intermediate in mildly affected area and Gobi area. The average silt content was the highest in severely affected area, followed by Gobi area and mildly affected area, with desert area having the lowest sand content. Conversely, the average sand content followed the opposite trend, in the order of desert area>Gobi area>mildly affected area>severely affected area. The soils in this area are primarily brown desert soils, characterized by four types: sandy soils, loamy sandy soils, sandy loams, and chalky sandy loams, with sandy loams being the most prevalent.

4.3 Changes in soil salinity

The spatial distribution of soil soluble salts in the study area and the soluble salt box plots of different watersheds are presented in Figures 5 and 6. The main ions present in the soils of Hotan Prefecture were K^+, Na^+, SO_4^{2-}, and Cl^-, indicating that the soils are primarily saline rather than alkaline. From the data shown in Figures 5a and 6a, it can be observed that the soil pH values in areas of heavy human impact across each watershed were lower than those in Gobi area and desert area. The overall regional soils exhibited alkaline characteristics, with pH values ranging from 7.63 to 9.59. Specifically, soils in the Yurungqash, Qaraqash, and Kriya river basins demonstrated weak alkalinity, with pH values ranging from 8.63 to 8.92. The soil pH values in the Gobi area and desert area of the lower reaches of the Celle and Niya river basins ranged from 8.93 to 9.59.

As depicted in Figures 5b and 6b, sample sites with higher EC in the Yurungqash and Qaraqash river basins were concentrated in Gobi and desert areas that were unaffected by human activities, with the highest recorded EC value of 22,200.00 μS/cm; in contrast, EC in other basins was relatively low, averaging 3620.00 μS/cm.

Figure 5c illustrates significant differences in the spatial distribution of K^+ and Na^+ across different ecosystems and anthropogenic influences, with concentrations ranging from 2.90 to 53,852.20 mg/kg. The concentration of Ca^{2+} varied from 2.40 to 4399.00 mg/kg, while the concentration of Mg^{2+} ranged from 3.70 to 4152.90 mg/kg (Fig. 5d and e). The concentrations of K^+, Na^+, Ca^{2+}, and Mg^{2+} were all notably lower in areas heavily influenced by human activities compared with those lightly influenced in the Yurungqash and Qaraqash river basins and Gobi and desert areas.

As shown in Figures 5f, there was a considerable spatial distribution pattern and concentration difference of Cl^- among each watershed. The minimum concentration of Cl^-in most plots was 24.80 mg/kg, with a small variation in areas heavily influenced by human activities (1205.80 mg/kg). The maximum Cl^- value in the lower reaches of Yurungqash and Qaraqash rivers and desert area reached 70,972.70 mg/kg. The spatial distribution and concentration differences of SO_4^{2-}, illustrated in Figures 5g, showed that the maximum concentration of SO_4^{2-} in the Gobi area reached 13,949.30 mg/kg. The concentration of HCO_3^-, shown in Figure 5i, exhibited a similar trend to that of pH changes, indicating significant variations in concentration within the Gobi and desert areas of Yurungqash and Qaraqash river basins (85.60–696.70 mg/kg). The high concentration in other watersheds was primarily concentrated in areas impacted by human activities.

(a) pH

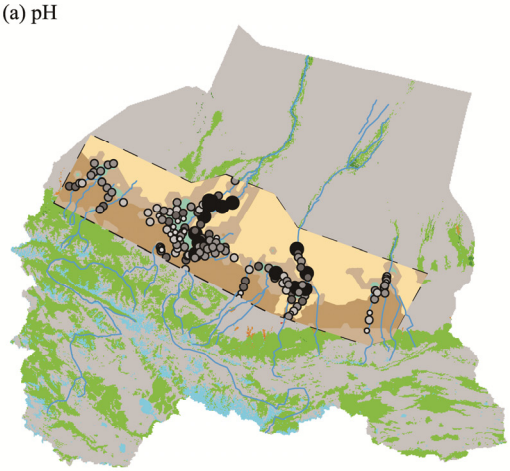

pH
- 7.63–8.06
- 8.07–8.33
- 8.34–8.62
- 8.63–8.92
- 8.93–9.59

(b) EC

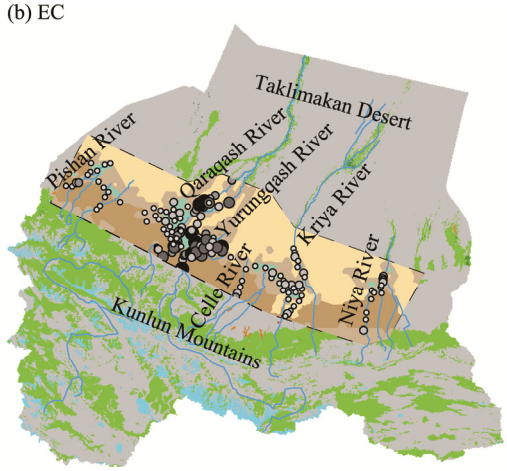

EC (μS/cm)
- 77.00–1282.00
- 1282.01–3960.00
- 3960.01–7640.00
- 7640.01–12,770.00
- 12,770.01–22,200.00

(c) K^++Na^+

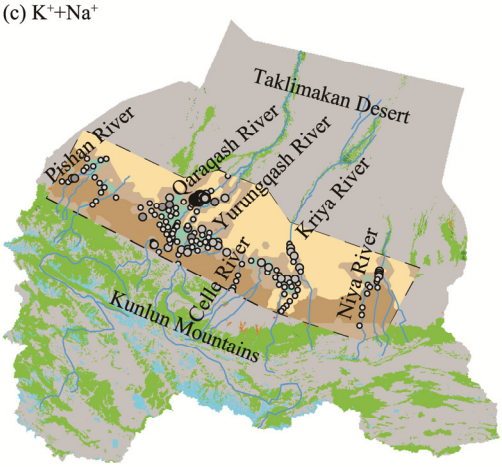

Concentration of K^++Na^+ (mg/kg)
- 2.90–949.00
- 949.01–3063.30
- 3063.31–6371.10
- 6371.11–26,509.40
- 26,509.41–53,852.20

(d) Ca^{2+}

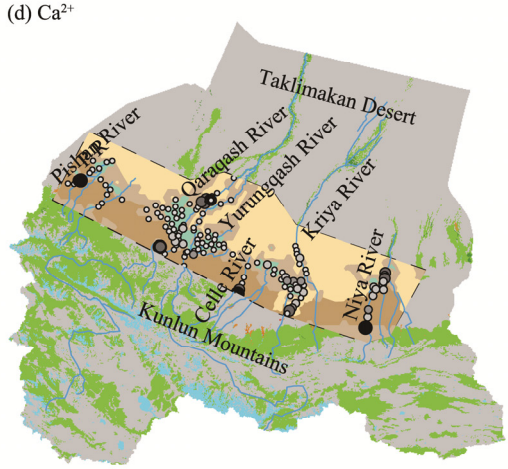

Concentration of Ca^{2+} (mg/kg)
- 2.40–140.40
- 140.41–447.40
- 447.41–1151.70
- 1151.71–2763.80
- 2763.81–4399.00

(e) Mg^{2+}

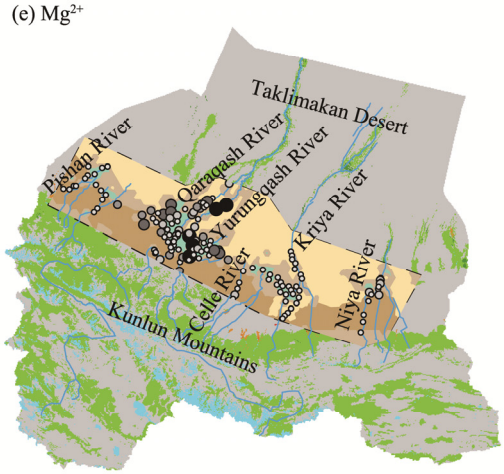

Concentration of Mg^{2+} (mg/kg)
- 3.70–166.70
- 166.71–505.00
- 505.01–1152.60
- 6371.11–26,509.40
- 26,509.41–53,852.20

(f) Cl^-

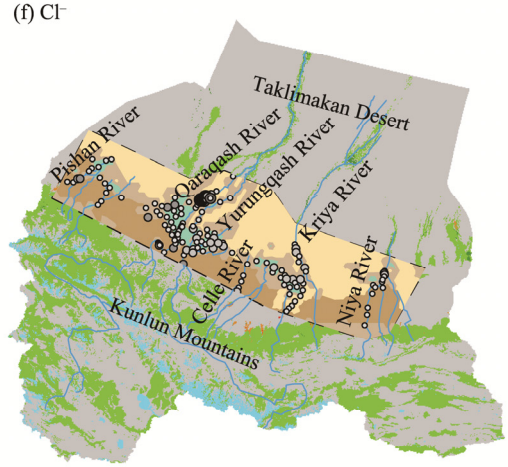

Concentration of Cl^- (mg/kg)
- 24.80–1032.00
- 1032.01–4099.70
- 4099.71–11,832.30
- 11,832.31–33,646.60
- 33,646.61–70,972.70

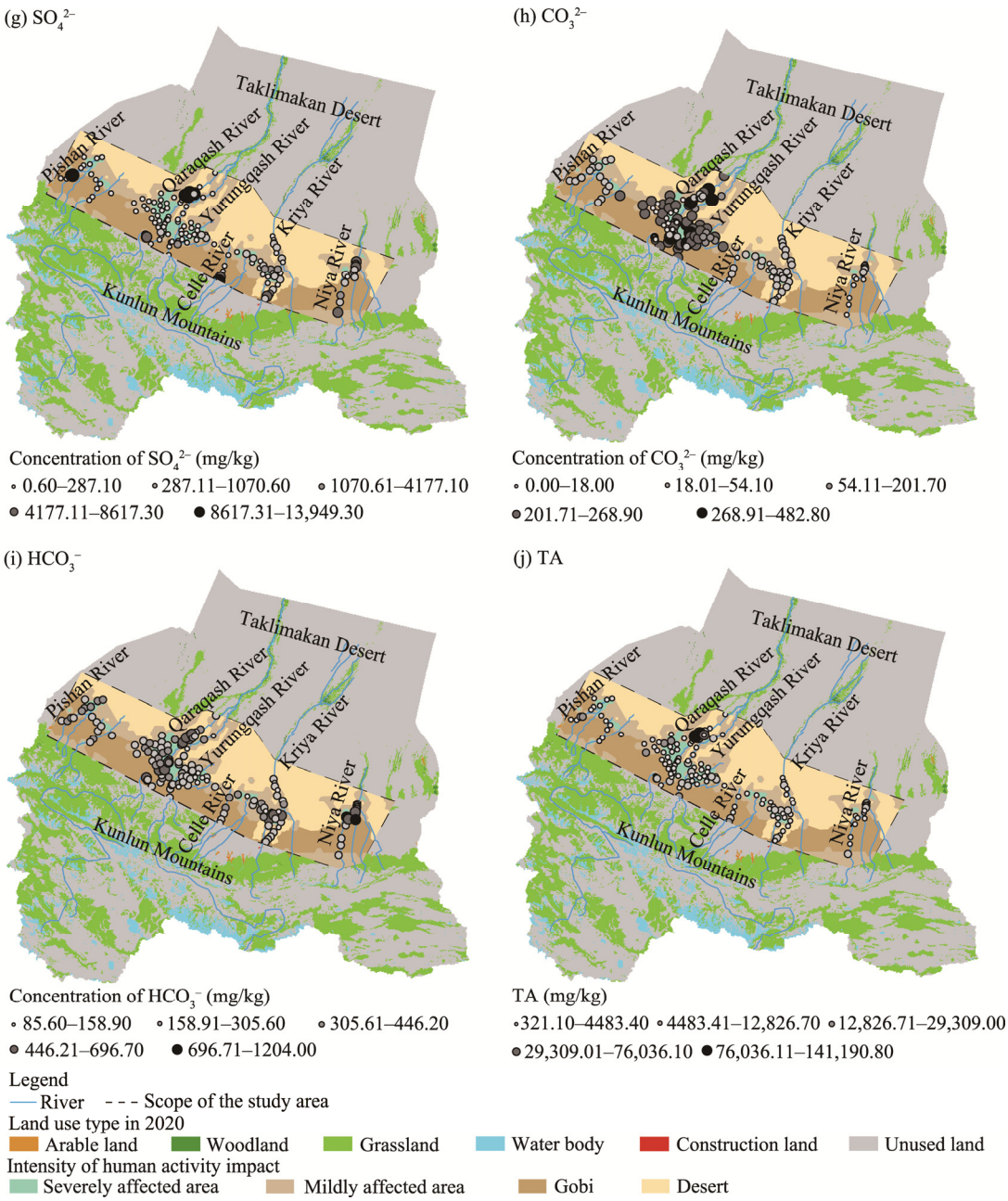

Fig. 5 Spatial distribution of soil soluble salt in the study area. (a), pH; (b), electrical conductivity (EC); (c), K^++Na^+; (d), Ca^{2+}; (e), Mg^{2+}; (f), Cl^-; (g), SO_4^{2-}; (h), CO_3^{2-}; (i), HCO_3^-; (j), total salt content (TA).

Figure 5h indicates that the trend of CO_3^{2-} concentration was similar to that of Mg^{2+}, characterized by lower concentration and minimal differences across each basin. The maximum concentration of CO_3^{2-} was 482.80 mg/kg in the Yurungqash and Qaraqash river basins, while the concentration in other basins ranged from 18.01 to 54.10 mg/kg. Finally, Figure 5j shows that the overall distribution of soluble salt content in the study area closely resembled that of Cl^-, with the transition zone between the downstream mildly influenced area and desert area of Yurungqash and Qaraqash river basins most closely matching the Cl^- distribution. The hypersaline plots were mainly concentrated in the transition zone between the mildly affected area and desert area of Yurungqash and Qaraqash river basins.

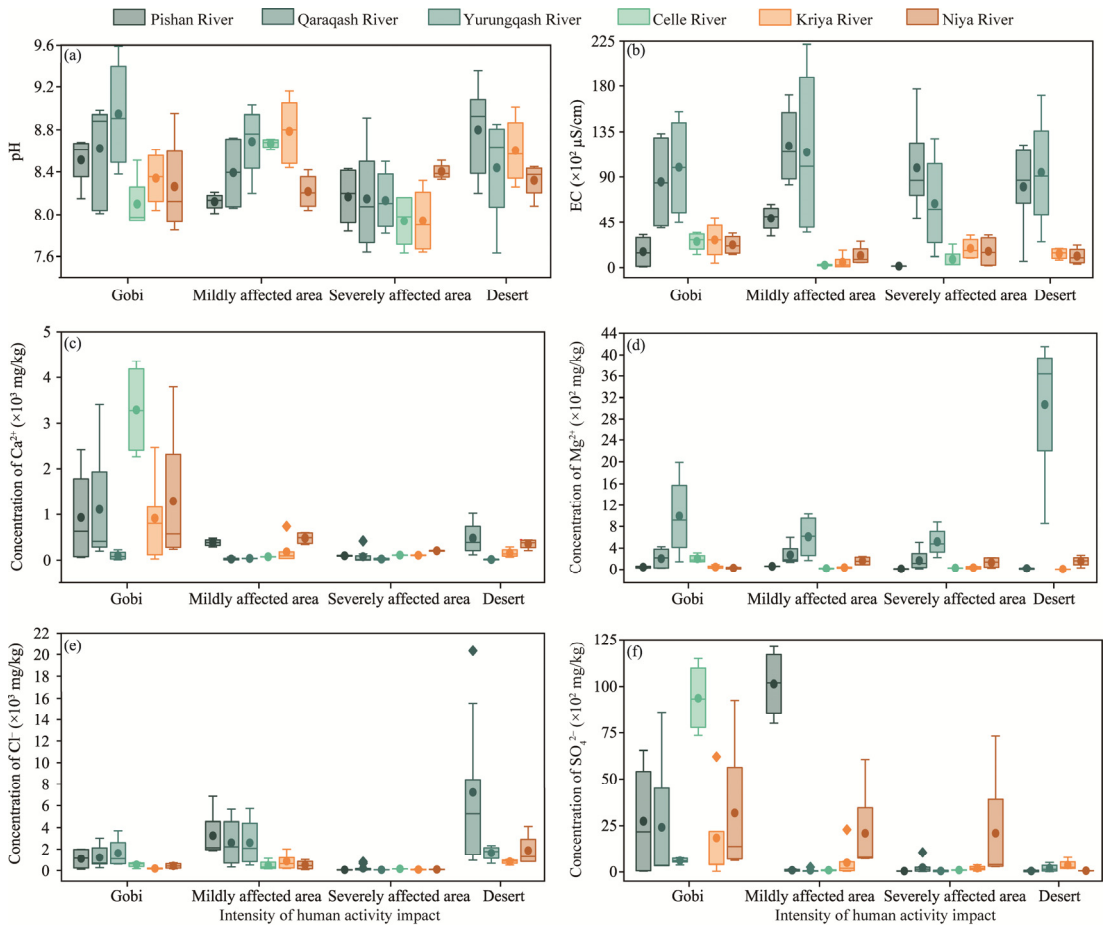

Fig. 6 Variation of soil soluble salt in typical watersheds of the study area. (a), pH; (b), EC; (c), Ca^{2+}; (d), Mg^{2+}; (e), Cl^{-}; (f) SO_4^{2-}. The upper and lower limits of the box plots represent the maximum and minimum values, the middle line represents median, the origin represents arithmetic mean, and the diamond-shaped block represents outlier.

4.4 Changes in soil nutrient content

The spatial distribution and box plot of soil nutrients in the study area are presented in Figures 7 and 8. The average soil content of OM was more than 10.00 g/kg, with the highest value reaching 31.10 g/kg in the area severely affected by human activities in each basin. In contrast, the content of OM was lower than 5.00 g/kg in Gobi and desert areas, with sample sites exhibiting high OM content primarily located in the anthropogenic impact area of Yurungqash and Qaraqash river basins.

Furthermore, the sample sites with high AN content were concentrated in the middle reaches of Yurungqash and Qaraqash river basins, as well as in the Pishan River and Niya River basins, with this trend becoming more pronounced when comparing different basins (Fig. 7a). The content of AN in the Gobi area of Pishan River and Niya River basins was lower, ranging from 440.01 to 894.00 mg/kg.

Additionally, Figures 7c and 8c indicate that the content of AP in the study area exhibited an increasing and then decreasing trend from west to east, with higher AP content observed in the Yurungqash and Qaraqash river basins, ranging from 440.01 to 894.00 mg/kg. The highest content of AP was found in anthropogenic impact area, while the content of AP in the other basins was lower, all below 50.00 mg/kg. Moreover, Figures 7d and 8d show that the content of AK was higher in the severely affected area of Qaraqash River and Niya River basins, ranging from 246.01 to 565.00 mg/kg.

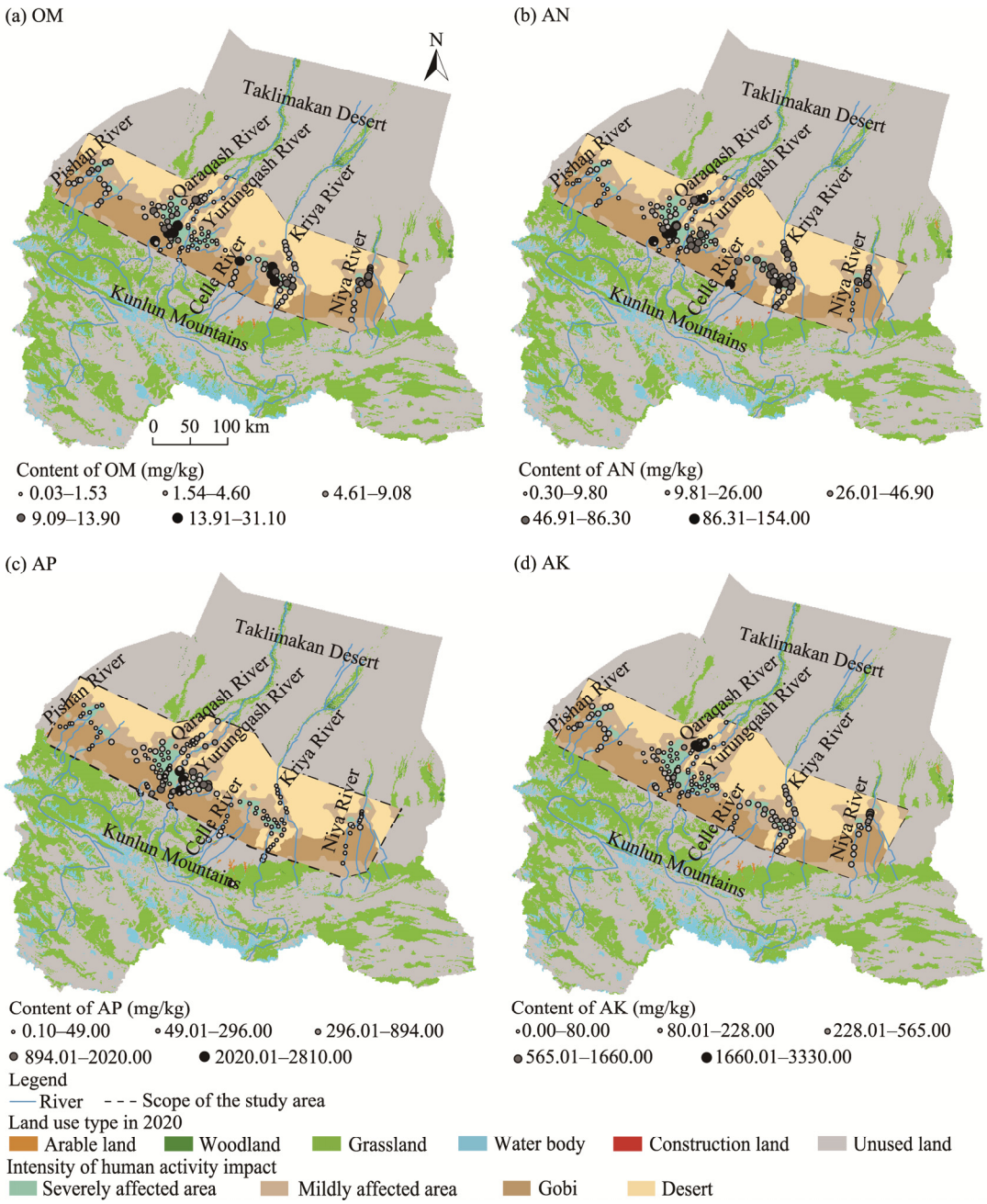

Fig. 7 Spatial distribution of soil nutrient in the study area. (a), organic matter (OM); (b), available nitrogen (AN); (c), available phosphorus (AP); (d), available potassium (AK).

The spatial distribution of salinization in Hotan Prefecture is depicted in Figure 9, revealing that the soils were primarily dominated by mildly and moderately salinized soils, accompanied by a small amount of severely and extremely salinized soils. The phenomenon of moderate to severe salinization was somewhat more prominent in Gobi area. The salt content of surface soil in areas with high-intensity anthropogenic activities in Hotan Prefecture was significantly lower, and the salinization problem in Gobi area was more severe than that in desert area. The anthropogenic impact area of Qaraqash and Yurungqash river basins was more densely populated than other areas in Hotan Prefecture and had frequent agricultural production activities, while this area showed lower degrees of soil salinization.

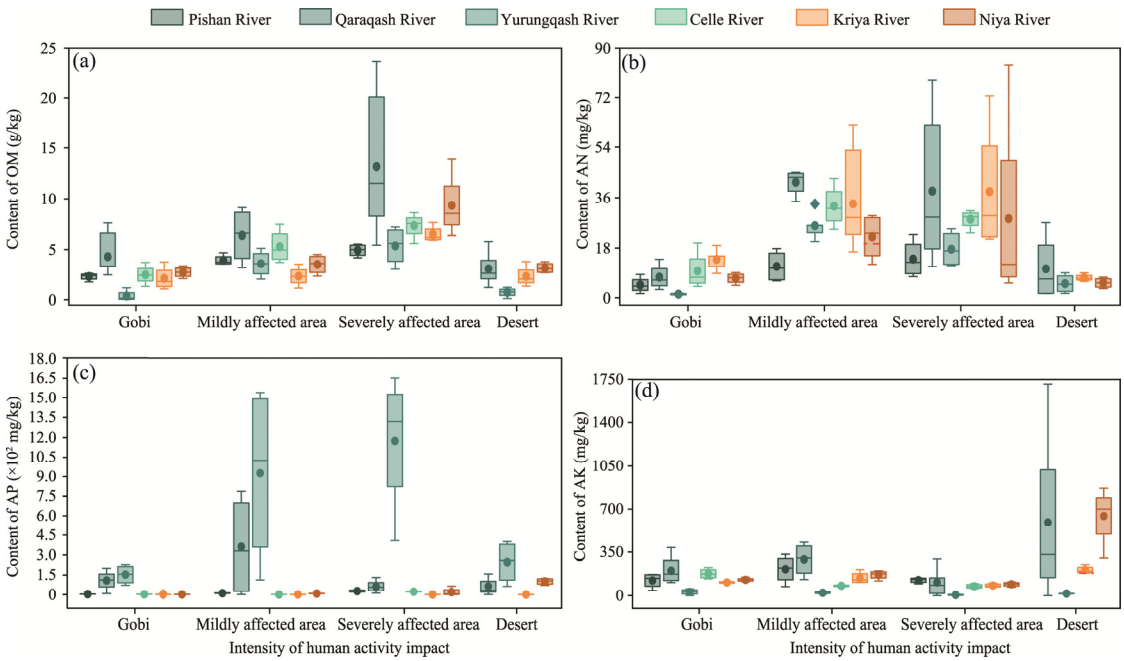

Fig. 8 Variation of soil nutrient in typical watersheds in the study area. (a), OM; (b), AN; (c), AP; (d), AK. The upper and lower limits of the box plots represent the maximum and minimum values, the middle line represents median, the origin represents arithmetic mean, and the diamond-shaped block represents outlier.

4.5 Correlation between water and soil

Taking the Yurungqash and Qaraqash river basins in Hotan Prefecture as an example, this study compared the salinity of groundwater, surface water, and soil salinity throughout the basins (Fig. 10). It was found that the type and content of soil salt ions were closely related to the type and content of ions in both surface water and groundwater. The anions were predominantly Cl^- and SO_4^{2-}, while the cations were predominantly K^+ and Na^+, indicating that the formation of salinization in Hotan Prefecture was directly influenced by the high degree of mineralization. This suggested that the formation of salinization in Hotan Prefecture was directly affected by the high mineralization of groundwater and surface water, and that the type of salinization was closely related to the composition of the parent rock from which the water source originated.

It was found that there was a highly significant negative correlation between soil OM, pH, and CO_3^{2-}. Additionally, there was a positive correlation between poorer soil nutrients and increased salinization (Fig. 11). In areas close to desert, where the impact of human activities was relatively weak, the nutrient content of Gobi and desert areas were significantly lower than that of the area influenced by human activities. This is true even though the soil texture is loose and the content of clay grains is low. This situation is related to the fact that the soil has been cultivated for many years under human influence, leading to a low water-holding capacity. This condition has been closely linked to anthropogenic farming and fertilizer application over the years. Combining the results of these experiments, the study summarized that the physical and chemical characteristics of soils in the study area were characterized by low soil water content, light and sandy textures, poor clay content, high soluble salts, and low nutrient content.

5 Discussion

Soil moisture is a crucial factor influencing the exchange of water, nutrients, and energy in the soil-plant-atmosphere continuum (Yin et al., 2021). It is restricted by geographic and climatic conditions, with all agricultural water sourced from artificial canals carrying glacial snowmelt

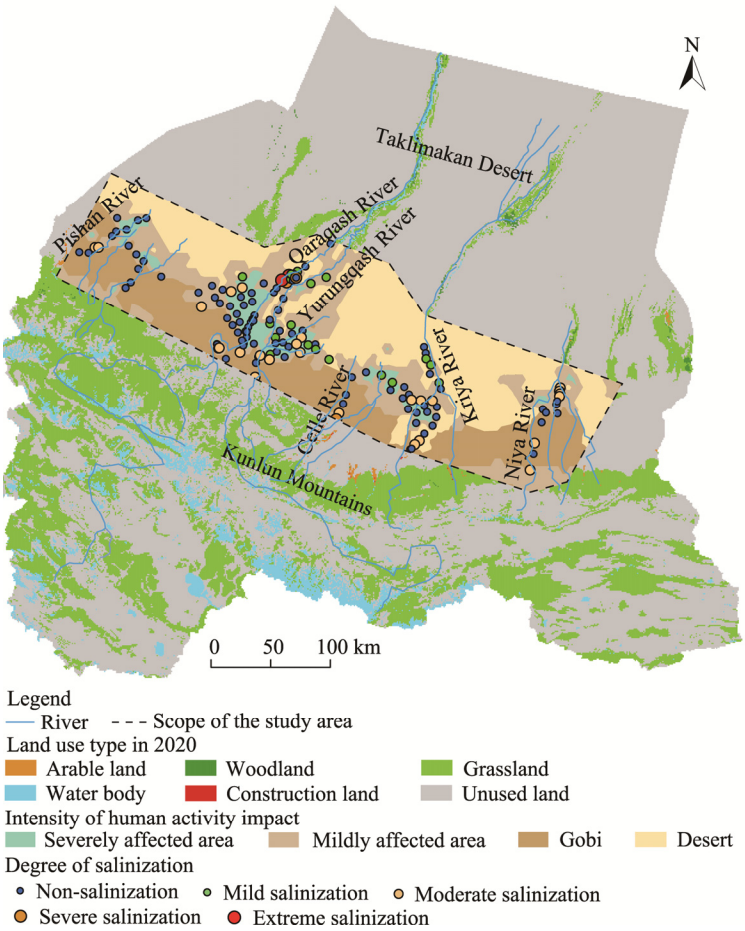

Fig. 9 Spatial distribution of soil salinity in the study area

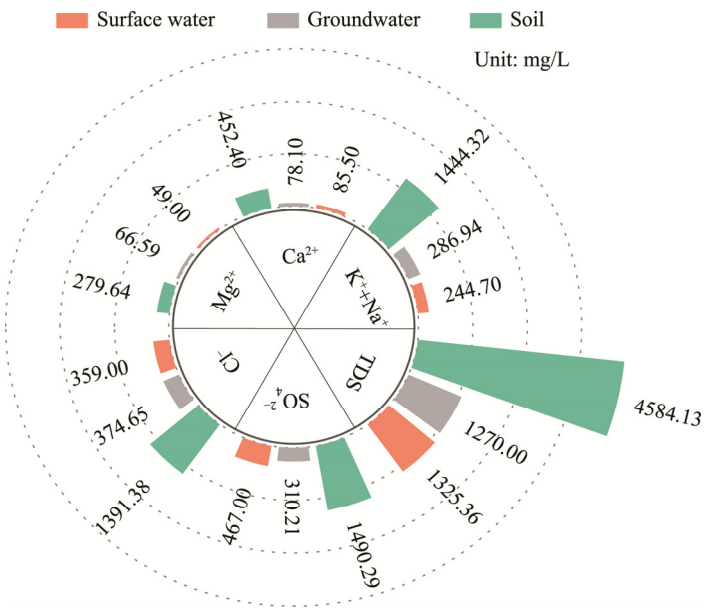

Fig. 10 Ion content of water and soil in the Yurungqash and Qaraqash river basins

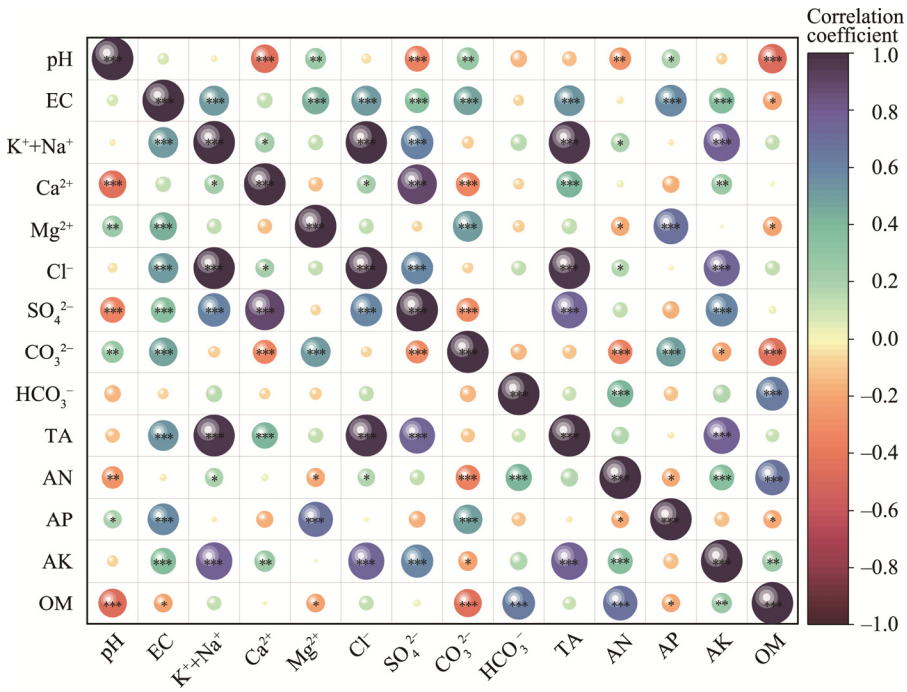

Fig. 11 Pearson correlation matrix of soil salinity and nutrient in the study area. *, P≤0.050; **, P≤0.010; ***, P≤0.001.

from the Kunlun Mountains and extracted groundwater recharge. According to statistical data (Su et al., 2021), the average annual flow of Qaraqash River is 21.64×10^8 m^3/a, and that of Yurungqash River is 22.88×10^8 m^3/a; these two rivers are significantly recharged, and the mineral composition of ice and snowmelt water influences the state of salt enrichment in the soil. The application of fertilizers in farming activities, the method of irrigation, and the type of crops planted all affect the distribution of soil salinity. This study aimed to reveal the spatial distribution pattern of soil salinization in Hotan Prefecture under the combined influence of natural factors (highly mineralized groundwater and surface water in this study) and human activities, as well as the degree of salinization under different levels of human intervention.

A small-scale study in Hotan Prefecture revealed that the type of soil salinization in Yutian County of Kriya River Basin was a chloride-sulfate composite, coinciding with the transition from chloride to a chloride-sulfate composite salinization in this area, as reported by Han et al. (2013). Compared with previous studies, there was a slight increase (less than 1.00%) in moderately salinized croplands and a decrease of approximately 1.50% in heavily salinized croplands in Hotan Prefecture (Zhuang et al., 2021b). In response to comprehensive changes in the shrinking spatial distribution of high-intensity anthropogenic activity area, the reduction of salinization hazard types, and the decrease in salinization content, the distribution pattern of salinized watersheds in Hotan Prefecture was explored. This was done under conditions of no significant change in natural precipitation (Yao et al., 2020), focusing on soil salinization responses in terms of both groundwater characteristics and human irrigation recharge and deep plowing activities.

The extensive use of glacial snowmelt through artificial canals and the extraction of groundwater recharge for agricultural and domestic purposes in Hotan Prefecture have led to the elevation of the groundwater table in the northwest area. A shallower groundwater table is more prone to triggering salt accumulation due to evaporation (Akter et al., 2021). In addition, numerous studies have confirmed the redistribution of soil salinity through water movement (Wang et al., 2014; Wang et al., 2016; Dong et al., 2021; Hui et al., 2022), which explains why soil salinization is more pronounced in desert area compared with anthropogenic area. This difference is primarily influenced by topography (e.g., groundwater flow from high to low), the

characteristics of Gobi and desert soils (e.g., coarse sand grains, high permeability, and rapid evaporation), and saline matrices. These factors contribute to the upwelling of salty groundwater under conditions of rapid evaporation, the accumulation of salts in shallow soils, and the phenomenon of secondary salinization (Wang et al., 2014; Qi et al., 2018; Yin et al., 2022).

This study clarified that water environmental factors play a key role in determining the spatial distribution of salinization. Additionally, the disturbance of water and soil environments by human activities affects the long-term evolution and spatial distribution of salinization (Li et al., 2017; Wang et al., 2021a). The impact of human activities on land use currently has a twofold perspective: large-scale farming and engineering activities. The two affairs often lead to salt accumulation due to traditional diffuse irrigation (Khaydar et al., 2021; Wang et al., 2021a; Yin et al., 2022; Bai et al., 2023), while rational farming practices and effective irrigation facilities can effectively mitigate salinization (Dong et al., 2020; Yao et al., 2023).

Recent studies have revealed the extent of anthropogenic intervention in oasis-desert ecosystems (Li et al., 2016a; He et al., 2020), indicating that changes in land-use practices, excessive extraction of groundwater, and inappropriate irrigation practices exacerbate the disruption of the water-salt balance (Zhang et al., 2014; Perri et al., 2018). Other researchers also using the Kriya River Basin of Hotan Prefecture as an example, found that monocropping triggers a soil nutrient imbalance, coupled with the excessive use of chemical fertilizers and pesticides in the production of food and cash crops. This leads to soil sloughing and a weakening of water retention properties, which exacerbates soil salinization to a certain extent (Zhuang et al., 2021b).

Activities such as farming accelerate the decomposition of OM by altering the soil microbial environment, resulting in a decrease in the contents of OM and AN in arable land (Zhang and Xu, 2023; Khan et al., 2024). At the same time, high topographic water sources carry salts to lowlands due to gravitational effects. Human activities indirectly change the physical properties of soil (e.g., permeability, water retention, and fertilizer retention) by adjusting the vegetation type, cover, and distribution, thereby affecting the accumulation of salts in the tillage layer and their migration to the edges of cultivated land and the transition zone of desert. Related studies found that in salinized areas with shallow groundwater, the combination of drip irrigation and ridge planting exerted a significant effect on vegetation restoration and saline soil reclamation (Dong et al., 2020). Therefore, it is crucial to enhance soil nutrients and thus alleviate salinization by changing farming systems and irrigation patterns (He, 2008; Huang et al., 2020).

In the development and utilization of saline soil, we suggest that in light saline soils, farmers should adopt deep tillage and increase the application of organic fertilizers, based on the local salt and nutrient distribution characteristics. For moderately saline soils, agricultural measures (e.g., mixed application of organic and inorganic fertilizers and planting salt-tolerant plants), biological interventions (such as straw mulching and increased application of microbial fertilizers), and water conservation strategies (such as water-saving irrigation) should be combined. However, for strongly saline soils, water conservation projects (such as salt discharge and salt washing) should be integrated to improve the utilization efficiency of saline soil and manage soil salinization.

In summary, this study clarifies the comprehensive influence of the natural environment (highly mineralized groundwater and surface water) and anthropogenic activities on soil salinization. It reveals the spatial distribution pattern of salinization under the influence of water environments and human activities in Hotan Prefecture, and it correctly identifies and diagnoses land desertification issues, exemplified by soil salinization. This understanding is a prerequisite for effective salinization reduction and prevention.

6 Conclusions

In this study, soil and surface water physical-chemical property parameters were collected and tested in six rivers (Pishan, Qaraqash, Yurungqash, Celle, Kriya, and Niya rivers) mainly developed in Hotan Prefecture. The soil water content of the watersheds indicated that human activity affected areas had higher moisture levels than Gobi and desert areas. In terms of pH,

human activity affected areas exhibited lower values compared with Gobi and desert areas. The human activity affected areas had lower soluble salt content than Gobi and desert areas. Additionally, this study determined that saline soils in Hotan Prefecture were mainly of chloride-sulfate type. The type of salinization was directly affected by the soil-forming parent rock, highly mineralized groundwater and surface water, while unreasonable human activities affected the degree of soil salinization. Weakly and moderately saline soils were mainly in the area impacted by human activities, and the transition zone between the areas impacted by human activities and desert was accompanied by a small amount of strongly and super-saline soils. the phenomenon of moderately and heavily salinized soils were more pronounced in Gobi. Although this study revealed that human activities mitigated soil salinization. However, what kind of farming activities (irrigation mode, cropping system) play a role in mitigating salinization requires long-term investigation and monitoring. Subsequent research should focus on water and salt transport patterns in the areas impacted by human farming activities to further reveal the intrinsic mechanism of human farming activities to mitigate salinization.

Conflict of interest

The authors declare that they have no known competing financial interests or personal relationships that could have appeared to influence the work reported in this paper.

Acknowledgements

This research was supported by the Tianfu Yongxing Laboratory Organized Research Project Funding (2023KJGG05) and the Geological Survey Project of Xinjiang Uygur Autonomous Region Geology and Mineral Exploration and Development Bureau (XGMB202356).

Author contributions

Conceptualization: LIU Yufang, YANG Qingwen; Methodology: LIU Yufang, YANG Qingwen; Formal analysis: PEI Xiangjun, LI Jingji, WANG Shuangcheng, HUANG Zhenfu, HAN Wei, ZHENG Tianliang; Writing - original draft preparation: LIU Yufang; Writing - review and editing: YANG Qingwen; Funding acquisition: YANG Qingwen. All authors approved the manuscript.

References

Akter F, Bishop T F A, Willem Vervoort R. 2021. Space-time modelling of groundwater level and salinity. Science of the Total Environment, 776: 145865, doi: 10.1016/j.scitotenv.2021.145865.

Bai J D, Wang N, Hu B F, et al. 2023. Integrating multisource information to delineate oasis farmland salinity management zones in southern Xinjiang, China. Agricultural Water Management, 289: 108559, doi: 10.1016/j.agwat.2023.108559.

Chen L J, Li C S, Feng Q, et al. 2019. Direct and indirect impacts of ionic components of saline water on irrigated soil chemical and microbial processes. Catena, 172: 581–589.

Chen Y L, Zhang Z S, Huang L, et al. 2017. Co-variation of fine-root distribution with vegetation and soil properties along a revegetation chronosequence in a desert area in northwestern China. Catena, 151: 16–25.

Daliakopoulos I N, Tsanis I K, Koutroulis A, et al. 2016. The threat of soil salinity: A European scale review. Science of the Total Environment, 573: 727–739.

Dong S D, Wan S Q, Kang Y H, et al. 2020. Prospects of using drip irrigation for ecological conservation and reclaiming highly saline soils at the edge of Yinchuan Plain. Agricultural Water Management, 239: 106255, doi: 10.1016/J.AGWAT.2020.106255.

Dong S D, Wan S Q, Kang Y H, et al. 2021. Different mulching materials influence the reclamation of saline soil and growth of the *Lycium barbarum* L. under drip-irrigation in saline wasteland in Northwest China. Agricultural Water Management, 247: 106730, doi: 10.1016/J.AGWAT.2020.106730.

Du Y Q, Liu X F, Zhang L, et al. 2023. Drip irrigation in agricultural saline-alkali land controls soil salinity and improves crop yield: Evidence from a global meta-analysis. Science of the Total Environment, 880: 163226, doi: 10.1016/j.sciotenv.2023.163226.

Duan Q T, Luo L H. 2021. Summary and prospect of spatialization method of human activity intensity: taking the Qinghai-Tibet

Plateau as an example. Journal of Glaciology and Geocryology, 43(5): 1582–1593. (in Chinese)

Fan W, Zhou J L, Zhou Y Z, et al. 2020. Water quality and health risk assessment of shallow groundwater in the southern margin of the Tarim Basin in Xinjiang, P. R. China. Human and Ecological Risk Assessment, 27(2): 483–503.

Han L, Gong L, Zhu M L. 2013. Soil nutrients and their relationship with water-salt properties in Yutian Oasis of the Keriya River Watershed. Journal of Xinjiang University (Natural Science Edition), 30(3): 257–261. (in Chinese)

He M D. 2008. Study on the variability of soil organic matter and entire nutrient—Take Hotan Oasis and the desert-oasis ecotone in Xinjiang as the example. MSc Thesis. Urumqi: Xinjiang Normal University. (in Chinese)

He M Z, Ji X B, Bu D S, et al. 2020. Cultivation effects on soil texture and fertility in an arid desert region of northwestern China. Journal of Arid Land, 12(4): 701–715.

Huang C B, Yan J, Ju J F, et al. 2020. Dynamic changes in soil properties and their relationships with wheat yield in the new reclaimed farmland in the southern Tarim Basin. Journal of Soil and Water Conservation, 34(2): 245–252. (in Chinese)

Hui R, Tan H J, Li X R, et al. 2022. Variation of soil physical-chemical characteristics in salt-affected soil in the Qarhan Salt Lake, Qaidam Basin. Journal of Arid Land, 14(3): 341–355.

Jiang Q S, Peng J, Biswas A, et al. 2019. Characterising dryland salinity in three dimensions. Science of the Total Environment, 682: 190–199.

Khan Z, Zhang K K, Khan M N, et al. 2024. Effects of biochar persistence on soil physiochemical properties, enzymatic activities, nutrient utilization, and crop yield in a three-year rice-rapeseed crop rotation. European Journal of Agronomy, 154: 127096, doi: 10.1016/j.eja.2024.127096.

Khaydar D, Chen X, Huang Y, et al. 2021. Investigation of crop evapotranspiration and irrigation water requirement in the lower Amu Darya River Basin, Central Asia. Journal of Arid Land, 13(1): 23–39.

Li X, Jiao Y, Dai G, et al. 2016a. Soil bacterial community diversity under different degrees of saline-alkaline in the Hetao Area of Inner Mongolia. China Environmental Science, 36(1): 249–260.

Li X, Xiong S M, Guo Z. 2016b. Improved mechanical properties in vacuum-assist high-pressure die casting of AZ91D alloy. Journal of Materials Processing Technology, 231: 1–7.

Li X J, Li Y Y, Wang B, et al. 2022. Analysis of spatial-temporal variation of the saline-sodic soil in the west of Jilin Province from 1989 to 2019 and influencing factors. Catena, 217: 106492, doi: 10.1016/j.catena.2022.106492.

Li X Y, Wang Y Q, Reynolds M E, et al. 2017. Long-term agricultural activity affects anthropogenic soil on the Chinese Loess Plateau. Journal of Arid Land, 9(5): 678–687.

Ministry of Ecology and Environment of the People's Republic of China. 2002. Technical Specifications Requirements for Monitoring of Surface Water and Waste Water (HJ/T 91-2002). [2024-01-01]. https://www.mee.gov.cn/ywgz/fgbz/bz/bzwb/jcffbz/200301/t20030101_66890.htm. (in Chinese)

Ministry of Housing and Urban-Rural Development of the People's Republic of China. 2009. Code for Investigation of Geotechnical Engineering (GB 50021-2001(2009)). [2024-05-18]. http://www.cday.cn/doc/GB50021-2009.pdf. (in Chinese)

National Health Commission of the People's Republic of China. 2006. Standards for Drinking Water Quality (GB5749-2006). [2024-01-26]. http://www.nhc.gov.cn/wjw/pgw/201212/33644.shtml. (in Chinese)

Perri S, Suweis S, Entekhabi D, et al. 2018. Vegetation controls on dryland salinity. Geophysical Research Letters, 45(21): 11669–116822.

Perri S, Suweis S, Holmes A, et al. 2020. River basin salinization as a form of aridity. Proceedings of the National Academy of Sciences of the United States of America, 117(30): 17635–17642.

Qi Z J, Feng H, Zhao Y, et al. 2018. Spatial distribution and simulation of soil moisture and salinity under mulched drip irrigation combined with tillage in an arid saline irrigation district, Northwest China. Agricultural Water Management, 201: 219–231.

Scanlon B R, Reedy R C, Gates J B. 2010a. Effects of irrigated agroecosystems: 1. Quantity of soil water and groundwater in the southern High Plains, Texas. Water Resources Research, 46(9): W09537, doi: 10.1029/2009WR008427.

Scanlon B R, Gates J B, Reedy R C, et al. 2010b. Effects of irrigated agroecosystems: 2. Quality of soil water and groundwater in the southern High Plains, Texas. Water Resources Research, 46(9): W09538, doi: 10.1029/2009WR008428.

Shokri-Kuehni S, Raaijmakers B, Kurz T. 2020. Water table depth and soil salinization: From pore-scale processes to field-scale responses. Water Resources Research, 56(2): e2019WR026707, doi: 10.1029/2019WR026707.

Su M, Wang H J, Tang W M. 2021. Analysis of the causes, water quality and value of Yurungqash River and Qaraqash River. Agricultural Development & Equipments, 11: 117–118. (in Chinese)

Tian C Y, Zhou H F, Liu G Q. 2000. The proposal on control of soil salinizing and agricultural sustaining development in 21's century in Xinjiang. Arid Land Geography, 23(2): 177–181. (in Chinese)

Wang Q M, Huo Z L, Zhang L D, et al. 2016. Impact of saline water irrigation on water use efficiency and soil salt accumulation

for spring maize in arid regions of China. Agricultural Water Management, 163: 125–138.

Wang R S, Wan S Q, Kang Y H, et al. 2014. Assessment of secondary soil salinity prevention and economic benefit under different drip line placement and irrigation regime in Northwest China. Agricultural Water Management, 131: 41–49.

Wang S J, Chen Q, Li Y, et al. 2017. Research on saline-alkali soil amelioration with FGD gypsum. Resources, Conservation and Recycling, 121: 82–92.

Wang W R, Chen Y N, Wang W H, et al. 2021a. Evolution characteristics of groundwater and its response to climate and land-cover changes in the oasis of dried-up river in Tarim Basin. Journal of Hydrology, 594: 125644, doi: 10.1016/j.jhydrol.2020.125644.

Wang W R, Chen Y N, Wang W H, et al. 2021b. Hydrochemical characteristics and evolution of groundwater in the dried-up river oasis of Tarim Basin, Central Asia. Journal of Arid Land, 13(10): 977–994.

Wang Z Y, Tan W J, Yang D Q, et al. 2021c. Mitigation of soil salinization and alkalization by bacterium-induced inhibition of evaporation and salt crystallization. Science of the Total Environment, 755: 142511, doi: 10.1016/j.scitotenv.2020.142511.

Yang H T, Li X R, Liu L C, et al. 2014. Soil water repellency and influencing factors of *Nitraria tangutorun* nebkhas at different succession stages. Journal of Arid Land, 6(3): 300–310.

Yang J, Huang X. 2021. The 30 m annual land cover dataset and its dynamics in China from 1990 to 2019. Earth System Science Data, 13(8): 3907–3925.

Yao J Q, Chen Y N, Zhao Y, et al. 2020. Climatic and associated atmospheric water cycle changes over the Xinjiang, China. Journal of Hydrology, 585: 124823, doi: 10.1016/j.jhydrol.2020.124823.

Yao R J, Gao Q C, Liu Y X, et al. 2023. Deep vertical rotary tillage mitigates salinization hazards and shifts microbial community structure in salt-affected anthropogenic-alluvial soil. Soil and Tillage Research, 227: 105627, doi: 10.1016/j.still.2022.105627.

Yin X W, Feng Q, Zheng X J, et al. 2021. Spatio-temporal dynamics and eco-hydrological controls of water and salt migration within and among different land uses in an oasis-desert system. Science of the Total Environment, 772: 145572, doi: 10.1016/j.scitotenv.2021.145572.

Yin X W, Feng Q, Li Y, et al. 2022. An interplay of soil salinization and groundwater degradation threatening coexistence of oasis-desert ecosystems. Science of the Total Environment, 806: 150599, doi: 10.1016/j.scitotenv.2021.150599.

Yu X, Lei J Q, Gao X. 2022. An over review of desertification in Xinjiang, Northwest China. Journal of Arid Land, 14(11): 1181–1195.

Zeng W Z, Xu C, Wu J W, et al. 2014. Soil salt leaching under different irrigation regimes: HYDRUS-1D modelling and analysis. Journal of Arid Land, 6(1): 44–58.

Zhang L N, Xu E Q. 2023. Effects of agricultural land use on soil nutrients and its variation along altitude gradients in the downstream of the Yarlung Zangbo River Basin, Tibetan Plateau. Science of the Total Environment, 905: 167583, doi: 10.1016/j.scitotenv.2023.167583.

Zhang N C. 2023. Status and characterization of surface water resources in the Hotan River Basin, Xinjiang. Groundwater, 45(2): 216–218. (in Chinese)

Zhang Z, Hu H, Tian F, et al. 2014. Groundwater dynamics under water-saving irrigation and implications for sustainable water management in an oasis: Tarim River Basin of western China. Hydrology and Earth System Sciences, 18(10): 3951–3967.

Zhao Q G. 1981. Analysis of Soil Physicochemical Features. Shanghai: Shanghai Science and Technology Press, 260. (in Chinese)

Zhao X M. 2018. Effects of simulated groundwater on water and salt characteristics of soil-*Tamarix chinensis* and tamarisk growth in the Yellow River Delta. PhD Dissertation. Tai'an: Shandong Agriculture University. (in Chinese)

Zheng C W, Deng X H, Li Z X, et al. 2024. Analysis of the spatial and temporal evolution of water resources conservation and human activity intensity in the Hexi Region of Gansu Province. Journal of Desert Research, 44(1):189–200. (in Chinese)

Zheng H, Wang X, Chen L, et al. 2018. Enhanced growth of halophyte plants in biochar-amended coastal soil: roles of nutrient availability and rhizosphere microbial modulation. Plant, Cell & Environment, 41(3): 517–532.

Zhuang Q W, Shao Z F, Huang X, et al. 2021a. Evolution of soil salinization under the background of landscape patterns in the irrigated northern slopes of Tianshan Mountains, Xinjiang, China. Ca, 206: 105561, doi: 10.1016/j.catena.2021.105561.

Zhuang Q W, Wu S X, Yang Y, et al. 2021b. Spatiotemporal characteristics of different degrees of salinized cultivated land in Xinjiang in recent ten years. Journal of University of Chinese Academy of Sciences, 38(3): 341–349. (in Chinese)